# CrystEngComm

Accepted Manuscript

ROYAL SOCIETY OF CHEMISTRY

www.rsc.org/crystengcomm

# Magnetic $CoFe_2O_4$ films with controllable dendritic arrays by a combined method of electrodeposition and anode activating

Hongcai He, Neng Qian, Ning Wang[1]

*State Key Laboratory of Electronic Thin Films and Integrated Devices and School of Microelectronics and Solid-State Electronics, University of Electronic Science and Technology of China, Chengdu 610054, P. R. China*

---

[1] Corresponding author, E-mail: ning_wang@uestc.edu.cn

## Abstract:

Cobalt ferrite ($CoFe_2O_4$, CFO) films with dendritic arrays, were prepared on $Pt/TiO_2/SiO_2/Si$ substrates by using a combined electrochemical method of electrodeposition and anode activating. Firstly, the $CoFe_2$ (CF) alloy films were electrodeposited from the solution of $Fe_2SO_4$ and $Co_2SO_4$ at room temperature. Then CFO films were prepared by anode activating and annealing the alloy films. Effects of preparation conditions on the crystalline structure, microtopography and magnetic properties of CFO films were investigated. Interestingly, it is different from the reported results that the smooth CFO films were obtained after annealing CF films in air condition even if without anodization, while controllable dendritic columnar arrays of CFO were observed after anode activating and annealing process. Anodization process was not necessary to form CFO films, but had an important effect on morphology of CFO films, and CFO films with desirable dentritic morphology could be adjusted by controlling anode-activating process parameters.

Keywords: cobalt ferrite, dendritic, electrodeposition, anode activating, magnetic

## Introduction

Ferrite thin films have been attracting increasing scientific interests because of their low cost, easily manufacturing and remarkable electric and magnetic properties. Among various ferrite materials, the spinel cobalt ferrite, $CoFe_2O_4$ (CFO), is a well-known hard magnetic material with wide applications due to its high coercivity, moderate saturation magnetization, remarkable chemical stability and mechanical hardness.[1, 2] It was also used in combination with ferroelectrics to produce magnetoelectric effect due its large magnetostriction.[3, 4] In addition, $CoFe_2O_4$ was also studied as potential materials for gas sensors[5] and photocatalyst[6] in recent years.

To meet more and more application requirements, much attention has been paid to how to control the microstructure and morphology of CFO films. CFO films could been prepared by quite a few techniques, such as sol-gel method[3], hydrothermal method[5], pulse laser deposition method[4] and sputtering method[7], electrodeposition method[8-10]. Among these ways, electrodeposition is reported as a promising and effective method to control microstructure and morphology of films by tuning many parameters such as deposition time, temperature, pH, current, potentials. However, it has been known that electrochemical deposition is often used for preparing metal[11, 12] or semiconductor films[13] but seldom used for the preparation of insulator like complex oxides. S.D. Sartale et. al.[8, 9] reported deposition of CFO thin films by an electrochemical deposition process, which is a combination of electrodeposition of CoFe2 alloy followed by its anodization. The anodization process at ambient temperature (~27 °C) was performed to form $CoFe_2O_4$ films. However, some results different from the previous reported results are observed in our experiments.

In this work, by using a combined electrochemical deposition process and anode activating method, CFO films with an oriented columnar morphology were prepared on Pt/$TiO_2$/$SiO_2$/Si substrates. Unlike S. D. Sartale's conclusion[8, 9], anodization process was not necessary to form CFO films, but had an important effect on morphology of CFO films. The smooth CFO films could be obtained after annealing $CoFe_2$ (CF) alloy films in air atmosphere even if without anode activating process, while dendritic arrays of CFO were observed after anode activating and annealing process. X-ray diffractometry (XRD), scanning electron microscope (SEM) were used to characterize the crystalline structure and morphology of the films, and a vibrating sample magnetometer (VSM) was used to measure the magnetic properties of the films. Effects of electrochemical deposition conditions on the morphology and magnetic properties of CFO films were investigated.

## Experimental Section

Electrochemical deposition[9, 14] was carried out in a three-electrode cell linked with electrochemical workstation (CHI660C, CH Instrument Co., ltd., China). The Pt/$TiO_2$/$SiO_2$/Si substrate, a platinum sheet and a saturated calomel electrode were used as the working electrode, the auxiliary electrode and the reference electrode, respectively. $CoFe_2$ (CF) alloy films were firstly deposited by the electrochemical deposition method on clean Pt/$TiO_2$/$SiO_2$/Si substrates referring to F. Lallemand and Y. Ye's work[15, 16]. The cobalt-iron electrolyte is a aqueous solution containing 25 mM

$CoSO_4$, 50 mM $FeSO_4$. The pH value of the solution was adjusted to 4 by using 5 mM $H_3BO_3$. Some organic additives including 4.4 mM saccharin, 0.28 mM sodium dodecyl benzene sulfonate (SOBS) and 10 mM sodium citrate were added to make the films more smooth and better. Saccharin was used as a brightening agent while sodium dodecyl benzene sulfonate as a surfacetant, and both of them could make the electrodeposited films brighter, smoother, more compact and more leveled. Even the presence of the saccharin could be helpful to the preferred orientations of the CoFe alloy deposition.[15] Sodium citrate could chelate metal ions in the suolution as a stabilizer to prevent the metal ions from oxidizing.[16] The solution was stirred in water bath at 28 °C for 3 h. The electrochemical deposition was carried out by applying constant potentials of -1.5 V~-2.1 V with the deposition time of 180 s. The distance between the substrate and the auxiliary electrode was fixed to 1.8 cm. After electrodeposition, the CF alloy films were treated with three methods as follows, (1) anode activating, (2) annealing, (3) anode activating and then annealing. For anode-activating, the CF film with the $Pt/TiO_2/SiO_2/Si$ substrate acts as an anode while a platinum sheet as a cathode. An aqueous solution of 1.5 M KOH was used as electrolyte. The alloy films were anode-activated by using a steady current of 0.1~0.2 A for 30 min. The annealing process was implemented in air at 550 °C or 600 °C for 3 h.

X-ray diffraction (XRD; Rigaku D/MAX-RB, Japan) with CuKα radiation was used for the phase analysis of the films under 40 kV and 30 mA. Scanning electron microscopy (SEM; INSPECTF FEI, Netherlands) was used to observe the microstructures. X-ray photoelectron spectroscopy (XPS, Kratos XSAM800, UK) was used to analyse the chemical state of elements in the films. The magnetization of films was characterized by a vibrating sample magnetometer (VSM, LakeShore 7410, USA).

## Results and discussion

Before obtaining CFO thin films, CF alloy films were firstly prepared by a usual electrodeposition method[17]. Fig. 1 shows the cross-section of the CF alloy film deposited with a potential of -2.1 V for 180 s at ambient temperature (27 $^{o}$C). The alloy film shows a columnar-like topography with a rough surface. The XRD pattern of the CF alloy film as Fig. 2a indicates that (110) preferential orientation of the CF alloy film was easily produced with the simple electrodeposition method. By changing deposition potential and deposition time, CF alloy films with different thickness can be obtained easily.

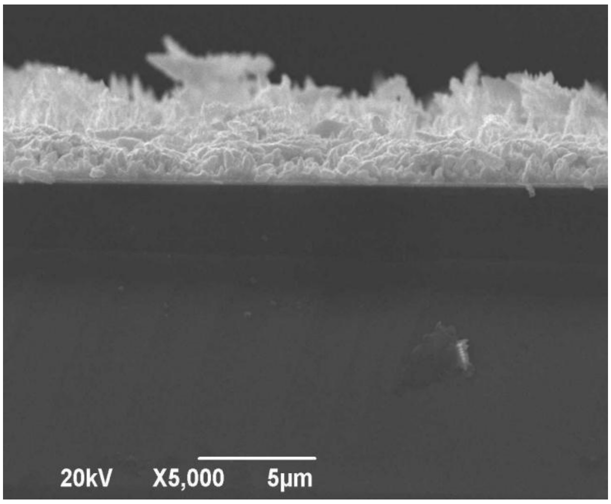

Fig. 1. SEM image of the CF alloy film prepared on the Pt/$TiO_2$/$SiO_2$/Si substrate with a deposition potential of 2.1 V and a deposition time of 180 s

The electrodeposited CF alloy films were treated by the following three methods, (1) anode activating, (2) annealed at 550 $^{o}$C or 600 $^{o}$C, (3) anode activating and then annealed at 550 $^{o}$C, and then four different samples were obtained. The XRD patterns of the four samples are shown as Fig. 2b, 2c, 2d, 2e, respectively. It is observed in Fig. 2b that the anode-activated $CoFe_2$ alloy film shows the (110) peak of $CoFe_2$ alloy without any obvious difference from the XRD pattern of the $CoFe_2$ alloy film as Fig. 2a. The result implies that the anode activating process without annealing was not able to oxidize the $CoFe_2$ alloy to cobalt ferrite. The films by annealing with or without anode activating show good XRD peaks of cobalt ferrites as Fig. 2c, 2d, 2e, respectively. The peaks are corresponding to (111), (220), (311), (400) , (422) and (511) planes of spinel cobalt ferrite polycrystals in accordance with standard PDF card ( PDF# 22-1086), which means that the CFO films were prepared by annealing $CoFe_2$ alloy films even if without anode activating. As a result, it is annealing process, but not anode-activating process that oxidizes alloy films to ferrite films. When the annealing temperature increases from 550 $^{o}$C to 600 $^{o}$C, the intensity of XRD peaks increases obviously, which suggests that the annealing process causes better crystallization. However, comparing the two CFO films from the processes annealing at the same temperature of 550 $^{o}$C with or without anode activating, the CFO film obtained by anodizing and then annealing a CF alloy film shows a little sharper and stronger XRD peaks than the CFO film by only annealing a CF film without anode activating process. This indicates that the anode-activating process has an effect on the formation and crystallization of CFO films.

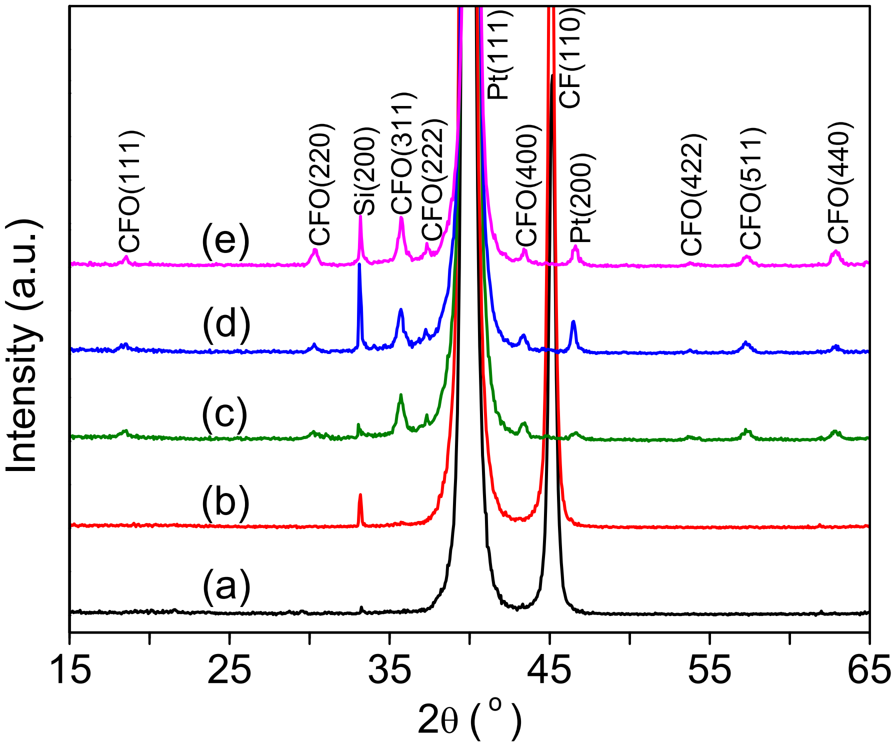

Fig. 2. XRD patterns of the films by different process:

(a) the CF alloy film by electrodeposition; (b) the anode-activated CF alloy film; (c) the film by annealing an alloy film at 550 °C without anode-activating; (d) the film by annealing an alloy film at 600 °C without anode-activating; (e) the film by anode-activating and then annealing an alloy film at 550 °C.

In order to confirm the above results, X-ray photoelectron spectroscopy (XPS) was used to analyse the chemical state of the Co element in the CF alloy film, the anodized CF alloy film and the CFO film, as shown in Fig. 3. The same atoms had different binding energy in different chemical environments. In details, the binding energy of the Co atoms in CF alloy, Co oxides and Co ferrite should be of a certain difference. However, XPS is a surface characteristic method and only detects quite a thin layer at the surface, while Co metal exposed to the air would be oxidized at the surface to form a surface oxide thin layer. As a result, the XPS pattern of Co metal commonly shows binding energy peaks of Co oxides but not Co metal. As shown in Fig. 3a, the Co $2p_{3/2}$ peak at 780.2 eV of the CF alloy film could be divided into two peaks of 781.3 eV and 780.0 eV, which correspond to CoO[18] and $Co_2O_3$[19], respectively. Figure 3b shows that the Co $2p_{3/2}$ main peak at 780.0 eV of the anode-activated CF alloy film just corresponds to $Co_2O_3$[19]. In addition, the spectral feature is similar to those reported by Tan[19] and Kim[20] for cobalt oxides, which shows a shoulder peak between 784.0 eV and 788.0 eV corresponding to the Co $2p_{3/2}$ satellite peak of $Co_2O_3$[19] or CoO[20]. The above XPS peaks corresponding to Co oxides should be caused by the thin oxide layer at the surface of the alloy films in air condition. Figure 3c shows that the Co $2p_{3/2}$ main peak at 779.9 eV of the film by anode-activating and annealing CF alloy film is corresponding to Co atoms in CFO film[18], as well as a shoulder peak between 784.0 eV and 788.0 eV is corresponding to the Co $2p_{3/2}$ satellite peak of $Co_2O_3$[19] or CoO[20]. The above XPS results indicate that CF alloy was not converted into CFO by anode-activating, which is in agreement with the XRD results in Fig. 2. According to the above XRD and XPS analysis, the anode-activating process did not oxidize CF alloy films to cobalt ferrite films, but the annealing process in air condition did. In other words, the annealing process is necessary to prepare cobalt ferrite films, but the anode-activating process is not.

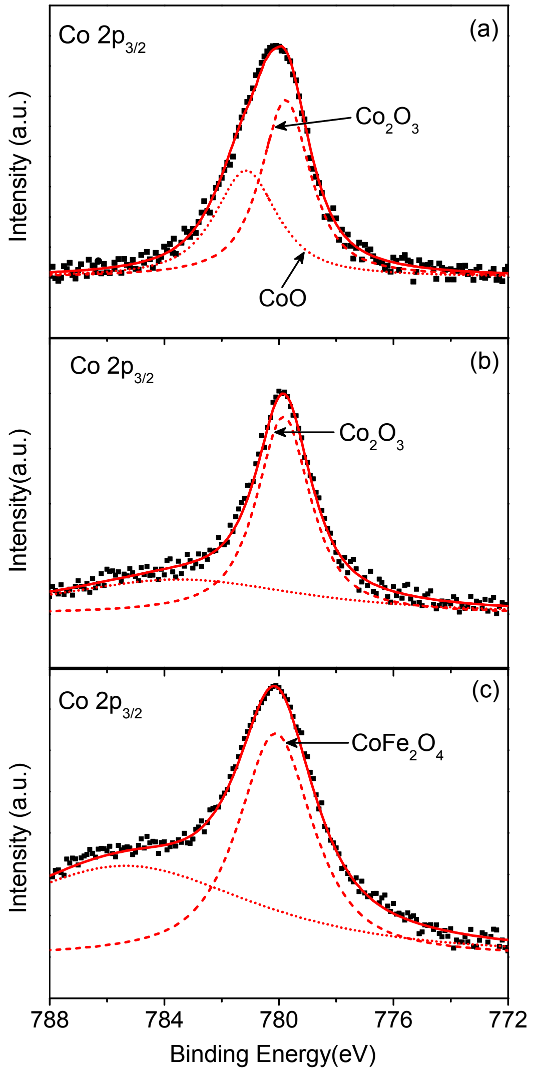

Fig. 3. XPS patterns of Co in the CF alloy film (a), the anode-activated CF alloy film (b) and the CFO films by anode activating and then annealing alloy film (c).

Figure 4 shows SEM cross-sectional images of CFO films prepared in different anode-activating conditions. The CFO film obtained by annealing CF alloy film without anode activating is a compact, smooth film with a thickness of about 3.5 μm as shown in Fig. 4a. Fig. 4b and 4c are SEM cross-sectional images of CFO films prepared with successively anode-activating and annealing from CF alloy films. The anode-activating process was carried out for 30 min at a voltage of 1.0 V, 1.7 V, with a corresponding anode-activating current of 0.098 A, 0.13 A, respectively. It is observed that the morphology of CFO films with anode activating is quite different from that of CFO films without anode activating, which indicates that the anode-activating condition plays an important role in determining the morphology of deposited CFO films. Obvious dendritic arrays are observed at the surface of the CFO films with anode activating, while there are still compact layers at the bottom of them. Fig. 4b shows the cross-sectional topography of the CFO film with an anode-activating voltage of 1.0 V. There is a bottom compact layer with a thickness of 600 nm, and a nonuniform dendritic array with a maximum height of about 2.9 μm and a maximum diameter of about 1.0 μm. When the anode-activating voltage increases to 1.7 V, the cross-sectional image of the obtained CFO film is shown in Fig. 4c with a bottom compact layer thickness of 500 nm and a dendritic maximum diameter of about 1.0 μm, while the maximum height of the dendritic structure increases to about 6.4 μm. Among the nonuniform dendritic arrays, there coexist some salient points, columnar dendrites, and even complex dendritic hierarchical structures. In a word, when the anode activating current increases, the height of the dendritic structure increases and the thickness of the bottom compact layer decreases. Thus, the anode-activating process influences the morphology of CFO films, and is proved as an effective method to control dendritic morphology of the deposited CFO films.

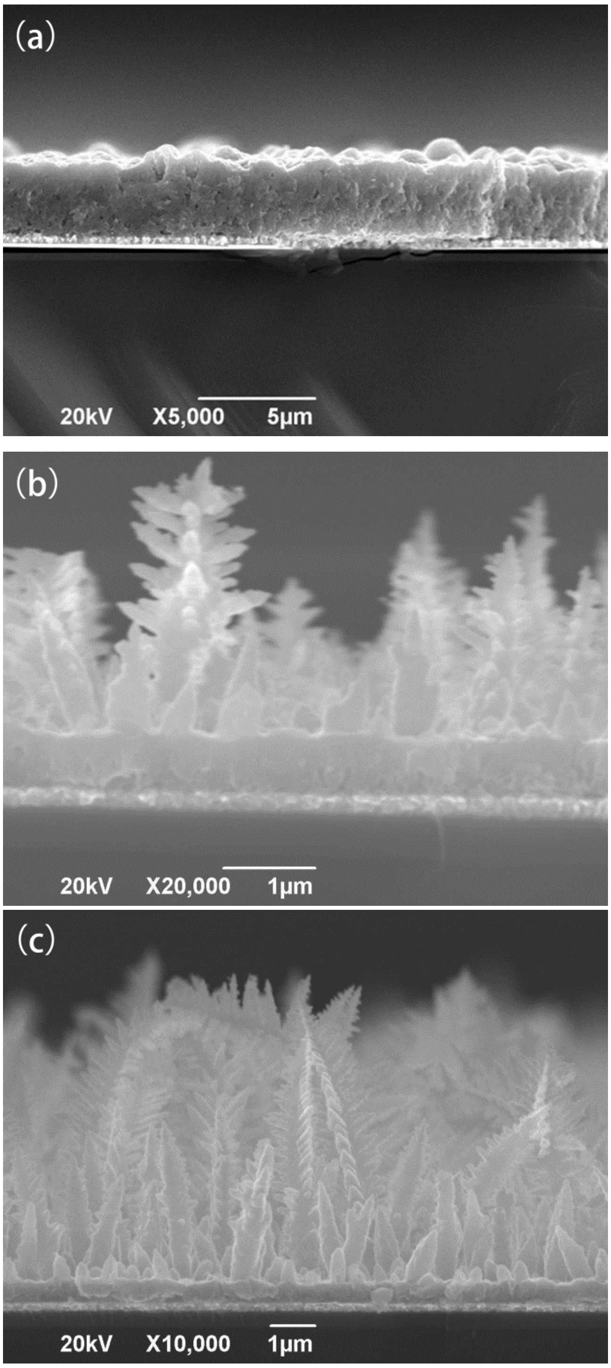

Fig. 4. SEM cross-sectional images of CFO films prepared by annealing CF alloy film without anode activating (a), and by annealing the CF alloy film anode-activated at voltage of 1.0 V (b), 1.7 V (c).

In order to illuminate the electrochemical growth process of CFO films, the evolution of morphology of films is shown in Fig. 5. Columnar CF alloy films were firstly obtained with a rough surface by the electrodeposition method as Fig. 5a. Actually electrochemical deposition is a common method to obtain metal or alloy films with a dendritic or columnar rough structure according to the classic diffusion-limited aggregation (DLA) model.[21, 22] According to this model, the metal nanoparticles deposite randomly onto the surface from electrolyte and diffuse on the surface of substrate. An attractive interaction between particles results in the fact that the particles adhere to the growing structure one by one and then form such a kind of dendrite and rough topography. Then when the CF alloy films are annealed in air condition for enough time, the $CoFe_2$ alloy films are fully oxidized as the following chemical equation: $CoFe_2 + 2O_2 = CoFe_2O_4$, and then CFO films are prepared and crystallized. The films become compact and smooth to reduce the surface energy during the oxidization and crystallization process, as shown as Fig. 5b.

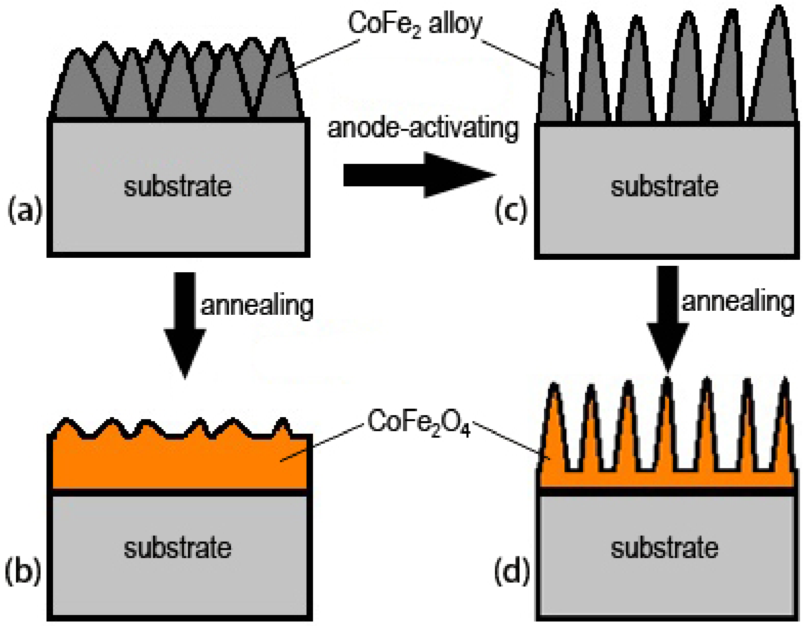

Fig. 5. The electrochemical growth process of CFO films

Electrochemical anodization is a feasible oxidization method[23], which was reported by S. D. Sartale et al. to oxide $NiFe_2$ alloy to deposit spinel nanocrystalline $NiFe_2O_4$ thin films[10]. However, when the CF alloy films were anodized in KOH solution according to the method reported by S. D. Sartale et al.[8, 10], the CF alloy films were not oxidized and converted to cobalt ferrite, as indicated in the XRD patterns (Fig. 2) and XPS results (Fig. 3), but the surface topography of the films was significantly changed into dendritic structures. Thus, here anode-activating was used to name this process as Fig. 5c. The formation of dendritic structure can be explained as a consequence of non-uniform electric field at the rough surface. During the anode-activating process, the rough CF film with the $Pt/TiO_2/SiO_2/Si$ substrate acts as an anode electrode. There are some sharp points at the surface of rough films. When applying an electric field, a high electric field will form at sharp points. As a result, the particles in electrolyte are preferentially aggregated to the sharp points under the high electric field. The non-uniform growth on the anode electrode leads to formation of dendritic structures. Finally, annealing processing in air condition is necessary to oxidize the anode-activated CF alloy films with dendritic structures, and dendritic CFO films are prepared. During annealing process, the CFO films tend to become smooth and compact in order to reduce surface energy. Consequently, a compact layer is formed at the bottom of the film, with a dendritic surface topograghy coming from the anode-activating process as shown in Fig. 4.

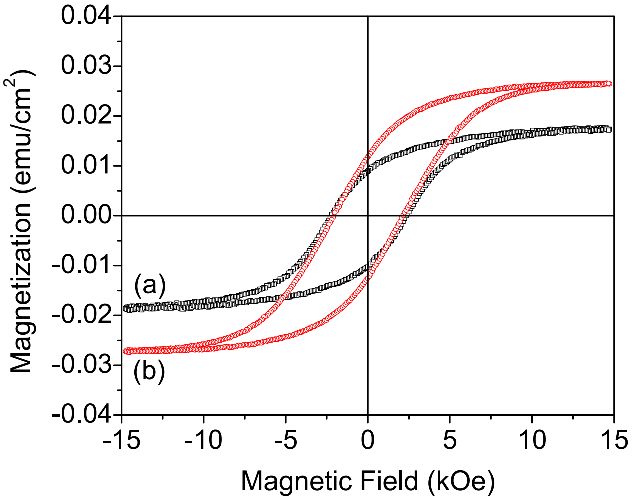

Fig. 6. Out-of-plane magnetic hysteresis loops of the CFO films by annealing the CF alloy film anode-activated at voltage of 1.0 V (a), 1.7 V (b).

Figure 6 shows the typical magnetic hysteresis loops of the dendritic CFO films which were measured with a magnetic field up to 15 kOe by applying magnetic fields perpendicular to the film plane (out of plane). The high magnetic coercive fields ($H_c$) of 1880 Oe and 1950 Oe are observed from the loops of the CFO films by annealing the CF alloy film anode-activated at voltage of 1.0 V and 1.7 V, respectively, which agrees with the coercivity of the CFO films by a sol-gel processing in our previous work [3]. The high $H_c$ of the films confirms further that the prepared films are cobalt ferrite films indirectly, but not CF alloy films which are soft magnetic materials with low coercivity. Though the CFO films show different topography and dendritic height, they are prepared by anodizing the CF alloy films with the same thickness. It is difficult to calculate the actual volume of the dendritic CFO films, and the magnetization of the CFO films is shown in emu/cm$^2$ to define the magnetization of film per unit area as shown in Fig. 6. It can be observed that the magnetization of the dendritic CFO films increases with increasing the height of dendritic structure, which can be attributed to the height difference of the dendritic array between the different CFO films.

## Conclusion

In conclusion, high-quality cobalt ferrite films with different topography can be prepared by a combined electrochemical method of electrodeposition and anode activating. Firstly, the $CoFe_2$ alloy films with columnar rough structure can be electrodeposited according to the classic diffusion-limited aggregation model. Then the smooth compact CFO films can be obtained by directly annealing CF alloy films in air condition without anode activating. Anode-activating processing can change the morphology and form dendritic CFO films as a consequence of non-uniform electric field at the rough surface, but it can not oxidize CF alloy films, which is interesting and different from the previous reports. The dendritic CFO films show a high coercivity and good magnetization. This study demonstrates that the controllable dendritic topography of cobalt ferrite films can be obtained by a simple electrochemical method and gives some helpful enlightenment to develop new application of cobalt ferrite films.

## Acknowledgement

This work was supported by National Natural Science Foundation of China

(51272035, 51272037, 51362026, 51472043), China-Japan International Cooperation Program Funds (No. 2010DFA61410 and 2011DFA50530), Program for New Century Excellent Talents in University (No. NCET-12-0097).

## References

1. V. Pillai and D. O. Shah, *J. Magn. Magn. Mater.*, 1996, **163**, 243-248.
2. Q. Song and Z. J. Zhang, *J. Am. Chem. Soc.*, 2004, **126**, 6164-6168.
3. H.-C. He, J. Wang, J.-P. Zhou and C.-W. Nan, *Adv. Funct. Mater.*, 2007, **17**, 1333-1338.
4. H. Zheng, J. Wang, S. E. Lofland, Z. Ma, L. Mohaddes-Ardabili, T. Zhao, L. Salamanca-Riba, S. R. Shinde, S. B. Ogale, F. Bai, D. Viehland, Y. Jia, D. G. Schlom, M. Wuttig, A. Roytburd and R. Ramesh, *Science*, 2004, **303**, 661-663.
5. C. Xiangfeng, J. Dongli, G. Yu and Z. Chenmou, *Sensor Actuat. B-Chem.*, 2006, **120**, 177-181.
6. Y. Fu, H. Chen, X. Sun and X. Wang, *Appl. Catal. B-Environ.*, 2012, **111**, 280-287.
7. J. G. Lee, K. P. Chae and J. C. Sur, *J. Magn. Magn. Mater.*, 2003, **267**, 161-167.
8. S. D. Sartale, G. D. Bagde, C. D. Lokhande and M. Giersig, *Appl. Surf. Sci.*, 2001, **182**, 366-371.
9. S. D. Sartale, C. D. Lokhande and V. Ganesan, *Phys. Status Solidi A*, 2005, **202**, 85-94.
10. S. D. Sartale, C. D. Lokhande, M. Giersig and V. Ganesan, *J. Phys.-Condens. Mat.*, 2004, **16**, 773-784.
11. Y. Ni, Y. Zhang, L. Zhang and J. Hong, *CrystEngComm*, 2011, **13**, 794-799.
12. Y.-J. Song, J.-Y. Kim and K.-W. Park, *Cryst. Growth Des.*, 2008, **9**, 505-507.
13. C. Han, J. Yang, C. Yan, Y. Li, F. Liu, L. Jiang, J. Ye and Y. Liu, *CrystEngComm*, 2014, **16**, 2823-2834.
14. J. B. Xue, W. Liang, X. G. Liu, Q. Q. Shen and B. S. Xu, *CrystEngComm*,

2012, **14**, 8017-8022.

15. F. Lallemand, L. Ricq, M. Wery, P. Berçot and J. Pagetti, *Appl. Surf. Sci.*, 2004, **228**, 326-333.
16. Y. Ye, Master's thesis, University of Electronic Science and Technology of China, 2002.
17. I. Shao, L. T. Romankiw and C. Bonhote, *J. Cryst. Growth*, 2010, **312**, 1262-1266.
18. N. S. McIntyre and M. G. Cook, *Anal. Chem.*, 1975, **47**, 2208-2213.
19. B. J. Tan, K. J. Klabunde and P. M. A. Sherwood, *J. Am. Chem. Soc.*, 1991, **113**, 855-861.
20. K. Kim, *Phys. Rev. B*, 1975, **11**, 2177-2185.
21. D. Bhattacharjya and I. Mukhopadhyay, *Langmuir*, 2012, **28**, 5893-5899.
22. T. A. Witten and L. M. Sander, *Phys. Rev. Lett.*, 1981, **47**, 1400-1403.
23. W. Lee and S.-J. Park, *Chem. Rev.*, 2014, **114**, 7487-7556.